

# **INVESTIGATION OF DYNAMIC FAILURE MECHANISM OF KENAF COMPOSITE USING SEM**

By:

**NUR LIYANA BINTI MOHAMAD FADZIELI**

(Matrix no: 120406)

Supervisor:

**Assoc. Prof. Dr Roslan Ahmad**

June 2017

This dissertation is submitted to

Universiti Sains Malaysia

As partial fulfillment of the requirement to graduate with honors degree in  
**BACHELOR OF ENGINEERING (MECHANICAL ENGINEERING)**



School of Mechanical Engineering

Engineering Campus

Universiti Sains Malaysia

## **DECLARATION**

This work has not previously been accepted in substance for any degree and is not being concurrently submitted in candidature for any degree.

Signed..... (Nur Liyana)

Date .....

## **STATEMENT 1**

This thesis is the result of my own investigations, except where otherwise stated. Other sources are acknowledged by giving explicit references. Bibliography/references are appended.

Signed..... (Nur Liyana)

Date .....

## **STATEMENT 2**

I hereby give consent for my thesis, if accepted, to be available for photocopying and for interlibrary loan, and for the title and summary to be made available outside organizations.

Signed..... (Nur Liyana)

Date .....

## ACKNOWLEDGEMENTS

Firstly, I would like to express my gratefulness towards God for the strength and good health for my own wellbeing to complete this thesis successfully.

I take this opportunity to express my deepest gratitude to Prof Madya Dr Roslan Ahmad, my advisor, for all the support and guidance he has given me throughout my undergraduate study and thesis work. His suggestions and constant encouragement helped me a lot. Besides that, I would also like to give my highest gratitude towards PHD candidate of School of Mechanical Engineering, USM, Mohd Sareh Aiman bin Hilmi, for his contribution throughout the process of completing this project. Also so much thank you to the all staff and technician at School of Mechanical Engineering, School of Aerospace Engineering and School of Material and Mineral Resources University Sains Malaysia for their help and guidance to use the facilities and machine provided in this school.

I also want to wish my special thanks towards my family and friends for their endless support physically and morally since the start of my study at USM up until I have completed this thesis. For all lecturer in USM, that taught me a very useful knowledge from the first year until now. Without them I might not be able to complete this task.

## CONTENTS

<b>DECLARATION</b> .....	i
<b>ACKNOWLEDGEMENTS</b> .....	ii
<b>CONTENTS</b> .....	iii
<b>LIST OF FIGURES</b> .....	v
<b>LIST OF TABLES</b> .....	vii
<b>LIST OF SYMBOLS</b> .....	viii
<b>LIST OF ABBREVIATIONS</b> .....	viii
<b>ABSTRAK</b> .....	ix
<b>ABSTRACT</b> .....	x
<b>CHAPTER 1</b> .....	1
1.1 Introduction.....	1
1.1.1 Kenaf Fiber Composite .....	1
1.1.2 Dynamic compression of Kenaf composite .....	3
1.1.3 Failure mechanism .....	4
1.2 Problem Statement .....	4
1.3 Objectives .....	5
1.4 Scope of Work .....	5
<b>CHAPTER 2</b> .....	6
2.1 Overview.....	6
2.2 Mechanical Properties of Kenaf Composite .....	6
2.3 Failure mechanism in dynamic compression.....	8
2.4 Concluding remark.....	10
<b>CHAPTER 3</b> .....	11
3.1 Overview.....	11

3.2 Material .....	11
3.3 Dynamic test .....	12
3.3.1 Basic principle of Split Hopkinson pressure Bar .....	12
3.3.2 Theory .....	13
3.3.3 Momentum trap technique .....	15
3.4 Scanning Electron Microscope .....	17
3.5 High speed camera.....	20
<b>CHAPTER 4</b> .....	<b>21</b>
4.1 Overview.....	21
4.2 Stress-Strain Graph .....	21
4.3 Effect of strain rate.....	24
4.4 Effect strain rate on failure mechanism morphology in dynamic compression.....	27
4.5 Failure at higher strain rate .....	34
4.6 Comparison failure between dynamic and static compression .....	36
<b>CHAPTER 5</b> .....	<b>41</b>
5.1 Conclusion .....	41
5.2 Future works .....	41
<b>REFERENCE</b> .....	<b>42</b>

## LIST OF FIGURES

Figure 1.1: Kenaf, kenaf fiber, and kenaf fiber-reinforced polylactic acid .....	2
Figure 1.2: The schematic diagram for Split Hopkinson Bar Pressure.....	3
Figure 2.1: The effect of KDC loading on moisture absorption of KDC/PLA composites[9].....	7
Figure 2.2: The SEM photographs of DTC1 specimen fracture at strain rate of 1150, (a) The interface between the, (b) Matrix plastic deformation fibers and matrix and softened [10].....	8
Figure 2.13 Micrographs of tensile failure sections of kenaf hybrid composites: (a) non- woven mat, (b) plain woven, and (c) unidirectional twisted yarns[11] .....	9
Figure 3.1: The diamond cutter to cut the kenaf with speed 2000rpm .....	11
Figure 3.2: Raw result of Strain against Time Graph obtained from SHPB Test.....	12
Figure 3.3: The schematic diagram for Split Hopkinson Pressure Bar.....	13
Figure 3.4: Raw result of Strain against Time Graph obtained from SHPB Test.....	13
Figure 3.6: The placed of momentum trapping .....	15
Figure 3.7: The flow of the momentum trapping when the incident tube suddenly hit the transfer flange, the incident tube moving towards the reaction mass. ....	16
Figure 3.8: The incident tube go back to the original position .....	16
Figure 4.1 : The example of raw data for the 1733s – 1.....	22
Figure 4.2: The stress-strain graph with different strain rate.....	23
Figure 4.3: The failure stress specimen with different strain rate.....	24
Figure 4.4: The failure strain specimen with different strain rate.....	25
Figure 4.5: The existing of void before the testing .....	26
Figure 4.6: The void arise cracking after the testing .....	26
Figure 4.7: The stress-strain curve with the different strain rate .....	27
Figure 4.8: The morphology image of the original kenaf composite specimen under SEM .....	28

Figure 4.9: The fiber splitting 45° from the original orientation at the 1003s – 1 .....	29
Figure 4.11: The failure mechanism on the kenaf composite with the five view at 851.9s – 1.....	31
Figure 4.12: The failure mechanism on the kenaf composite with the five view at 1003s – 1.....	32
Figure 4.13: The failure mechanism on the kenaf composite with the five view at 1593.99s – 1.....	33
Figure 4.14: The flow of the failure by using high speed camera .....	34
Figure 4.15: The stress versus strain graph for static and dynamic compression.....	36
Figure 4.16: The comparison failure mechanism of static and dynamic compression.....	39
Figure 4.17: The fibre discloted to misaligned at the 12s – 1 .....	40

## LIST OF TABLES

Table 3.1: The specification of scanning electron microscope Model S-3700N	28
Table 3.2: The description of high speed camera 2	29
Table 4.1: The detail properties for the compression testing	33
Table 4.2 : The properties for the dynamic and static compression	43



## LIST OF SYMBOLS

LIST OF SYMBOLS	SYMBOL DESCRIPTION	UNIT
d	Diameter	mm
L	Length	mm
t	Time	s
$\sigma$	Stress	MPa
$\varepsilon$	Strain	dimensionless
$\dot{\varepsilon}$	Strain Rate	$s^{-1}$
$\rho$	Density	$kg/m^3$

## LIST OF ABBREVIATIONS

SHPB	Split Hopkinson Pressure Bar
SEM	Scanning Electron Microscope

## ABSTRAK

Ujian dinamik telah dijalankan dengan menggunakan alatan Split Hopkinson Pressure Bar (SHPB). Ujian ini dijalankan ke atas Kenaf komposit pada kadar terikan  $872s^{-1}$ ,  $1003s^{-1}$  dan  $1594s^{-1}$  bagi setiap saat. Graf tekanan-terikan dengan pelbagai kadar terikan telah diplot dan dibincangkan. Oleh itu, ujian statik pada bahan yang sama telah dijalankan ke atas Universal Testing Machine (UTM) dan hasilnya dibandingkan dengan ujian dinamik dengan membezakan keadaan mekanisme kegagalan. Kegagalan spesimen daripada semua ujian telah disiasat menggunakan Scanning Electron Microscope (SEM). Hasil untuk graf tegasan-terikan menunjukkan tekanan kegagalan maksimum semakin meningkat bergantung kepada kadar tekanan yang semakin meningkat. Pada mampatan dinamik, mekanisme kegagalan yang lebih progresif pada kadar terikan yang lebih tinggi. Mod kegagalan awal pada pembebanan dinamik kegagalan yang berlaku bermula dari matriks retak sedangkan permulaan kegagalan pada mampatan statik mod ialah pemisahan serat dan matrik.

## ABSTRACT

The dynamic tests were carried out by using Split Hopkinson Pressure Bar (SHPB) apparatus. The test were conducted on Kenaf composite at strain rates of  $872s^{-1}$ ,  $1003s^{-1}$  and  $1594 s^{-1}$  per sec. The stress strain curves at various strain rate were plotted and discussed. Consequently, a quasi-static test on similar material were conducted on Universal Testing Machine (UTM) and the result were compared to the dynamic tests regarding to the failure mechanism. Failure of specimen from all tests were investigated using a Scanning Electron Microscope (SEM). The result for the stress-strain graph show the maximum failure stress is increasing depend on the increasing strain rate. At the dynamic compression, the failure mechanism more progressive at the higher strain rate. The initial failure mode at the dynamic loading the failure occur starting at the matrix cracking whereas at the static compression the initial debonding mode presented.

## CHAPTER 1

### INTRODUCTION

#### 1.1 Introduction

##### 1.1.1 Kenaf Fiber Composite

Kenaf is one of natural fiber that is very useful for industries and researchers. This material can be utilize in different polymer composites due to various application. In addition, kenaf fiber offers the advantages of being biodegradable, of low density, non-abrasive during processing and environmentally safe [1]. The interesting features of kenaf fibers are the low cost, lightweight, renewability, biodegradability and high specific mechanical properties. Kenaf has a bast fibre which contains 75% cellulose and 15% lignin and giving the advantages of being biodegradable and environmentally safe [2]. Among natural fibre composites, kenaf fibre reinforced composites have found imaginable applications for mobile phone shells consisting 15–20% .kenaf fibres [3]. Another example in the automobile industry is the Toyota RAUM, which is equipped with a spare tire cover made of kenaf fibre composites [4]. Kenaf is the one of the most widely used natural fibers which has been successfully incorporated in variety of application.

Historically, kenaf has been used as a cordage crop to produce twine, rope and sackcloth. Kenaf composite has good mechanical properties and can grow quickly, rising to as height as 4-5 m in within 4-5 month growing season with the kenaf's stalk diameter of 25-35 mm[5] . It means that kenaf fibre composite would give the opportunity to produce products similar to that material of wood, but it takes only 150 days to harvest. There is more variation of the fiber length at the top of the stalk. Also, the longest fibers are located at the top. The different parts of the plant of kenaf have a different chemical

and physical properties. That is, the chemical compositions and fiber properties of plant tissue taken from the roots, stem, trunk and leaves are different and are also different at different stages of the growing season. From figure 1.1 the plant of kenaf and developing a new composite material which is kenaf fiber-reinforced polylactic acid. This material boasts the highest biomass-based content (90% of resin content, excluding inorganics) of any bioplastic for electronic equipment.

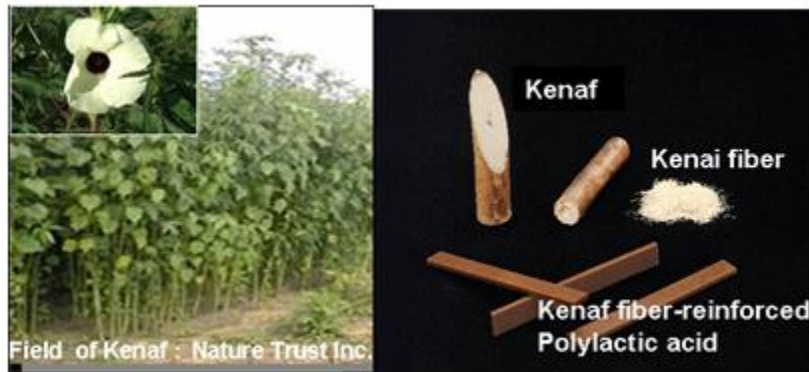


Figure 1.1: Kenaf, kenaf fiber, and kenaf fiber-reinforced polylactic acid

On the other hand, different parts of a plant have different chemical and physical properties. That is, the chemical compositions and fiber properties of plant tissue taken from the roots, stem, trunk and leaves are different and are also different at different stages of the growing season. Fiber length increases in the early part of the growing cycle, and then decreases again for the plant matured [6]. This may be an advantage in harvesting of the fiber before the plant matures.

### 1.1.2 Dynamic compression of Kenaf composite

The understanding of materials behavior is an important area of study in engineering. Material behave differently when subjected to different loading and rates. Hence, the characterization of material is a continuing study especially on a new material to obtain the stress-strain behavior and its fracture or failure behavior. There are two category of tests which involve material deformation that is static test and dynamic test. There are also several type of deformation like low strain rates and high strain deformation. Many applications experienced a high strain rates deformation like drop object, explosions, penetrations, and engineering application like bullet proof armors, and crash test of vehicle

The Split-Hopkinson pressure bar is an apparatus for dynamic testing of material in compression loading at various strain rate can be obtained. The dynamic properties such as modulus, maximum failure stress, and maximum failure strain can be deduced from the stress-strain curve. A schematic diagram of the SPHB arrangement is shown in figure 1.2.

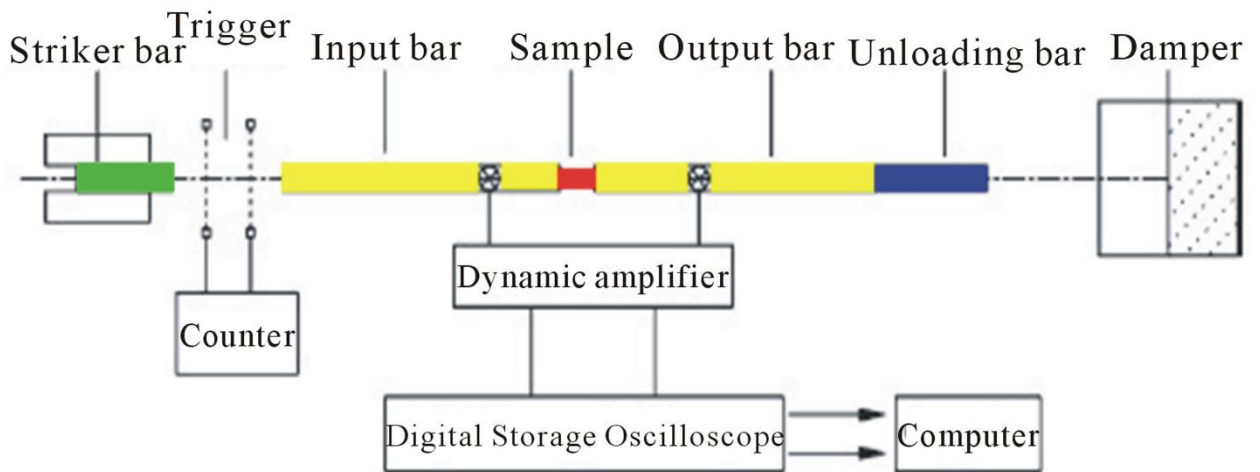


Figure 1.2: The schematic diagram for Split Hopkinson Bar Pressure

### **1.1.3 Failure mechanism**

The knowledge of identify failure mechanism is important in the world of engineering since it can cause defeat in design of application. The materials engineer often plays a lead role in the analysis of failures, whether a component or product fails in service or if failure occurs in manufacturing or during production processing. In any case, one must determine the cause of failure to prevent future occurrence, and/or to improve the performance of the device, component or structure. The term composites now covers a wide range of existing and emerging engineering materials. Different types of composite exhibit a wide variety of failure mechanisms. However, a common feature of these diverse materials is their inhomogeneous and frequently markedly for this experiment, focus more in dynamic compressive test. The basic failure mechanisms at the microscopic level include tensile, compressive or shear fracture of the matrix, bond failure of the fiber-matrix interface and tensile or compressive failure of the fibers. In this thesis, the experiment conduct dynamic compression on the kenaf composite. The majority of the criteria proposed identify the following failure modes, fiber fracture, transverse matrix cracking, shear matrix cracking. [7]

### **1.2 Problem Statement**

Natural fiber is usually used as reinforcement in polymeric materials, and short fibers are commonly used for non-structural applications. However, the lack of knowledge on the dynamic failure natural fiber reinforced polymeric materials, especially kenaf fiber has limited its usage in Malaysia. The knowledge is rarely discussed by the researcher. This work presents the experimental results of failure mechanism of kenaf fiber composite under dynamic compression testing.

### **1.3 Objectives**

The main purposes of this project is to investigate the dynamic failure mechanism of kenaf composite. The main of objectives are:

- 1) To characterize the compressive properties of kenaf composite under static and dynamic compression loading
- 2) To identify the failure mechanism of the kenaf fiber with different strain rate
- 3) To compare the static and dynamic failure mechanism of kenaf composite

### **1.4 Scope of Work**

- 1) The material used for the test is unidirectional kenaf composite with the composition of 70% fiber and 30% matrix. The kenaf in the circle shape with diameter of 12mm
- 2) Static test used Universal Testing Machine while dynamic utilize by Split Hopkinson Pressure bar using various strain rate
- 3) Failure mode was obtained by using Scanning Electron Microscope



## **CHAPTER 2**

### **LITERATURE REVIEW**

#### **2.1 Overview**

This chapter presents the interesting work of various researchers about the kenaf properties and dynamic compression loading. Their summary of significant findings and suggestions will be discussed.

#### **2.2 Mechanical Properties of Kenaf Composite**

It was reported by (Ishak, Leman, Sapuan, Edeerozey, & Othman, 2010) kenaf fibre has high potential to be used for composite reinforcement in biocomposite material. It is made up of an inner woody core and an outer fibrous bark surrounding the core. Results showed that the composites reinforced with kenaf bast fibre had higher mechanical properties than kenaf core fibre composites. The results also showed that the optimum fibre content for achieving highest tensile strength for both bast and core fibre composites was 20%wt. It was also observed that the elongation at break for both composites decreased as the fibre content increased. For the flexural strength, the optimum fibre content for both composites was 10%wt while for impact strength, it was at 10%wt and 5%wt for bast and core fibre composites respectively. The conclusion for this literature review is the higher cellulose content, the smaller fibre diameter and the longer fibre significantly increase the mechanical properties of the composite [8]

Experimented by (Tawakkal, Talib, Abdan, & Ling, 2012) the tensile elongation at the break point and during flexural and impact testing and on the water absorption was investigated. The specimen of kenaf derived cellulose and filled polyactic acid were combined by using melt blending and compression molding. From the flexural testing, the strength of these composite was improved compared to the neat PLA because of well-formed interface that allows better stress transfer from matrix to the fiber. The rough surface of the KDC may improve the adhesive characteristics and thus improve the stress transfer during applied load. The adding KDC did not significantly contribute to the total impact strength of the composite. However, increasing the adding weight of KDC will

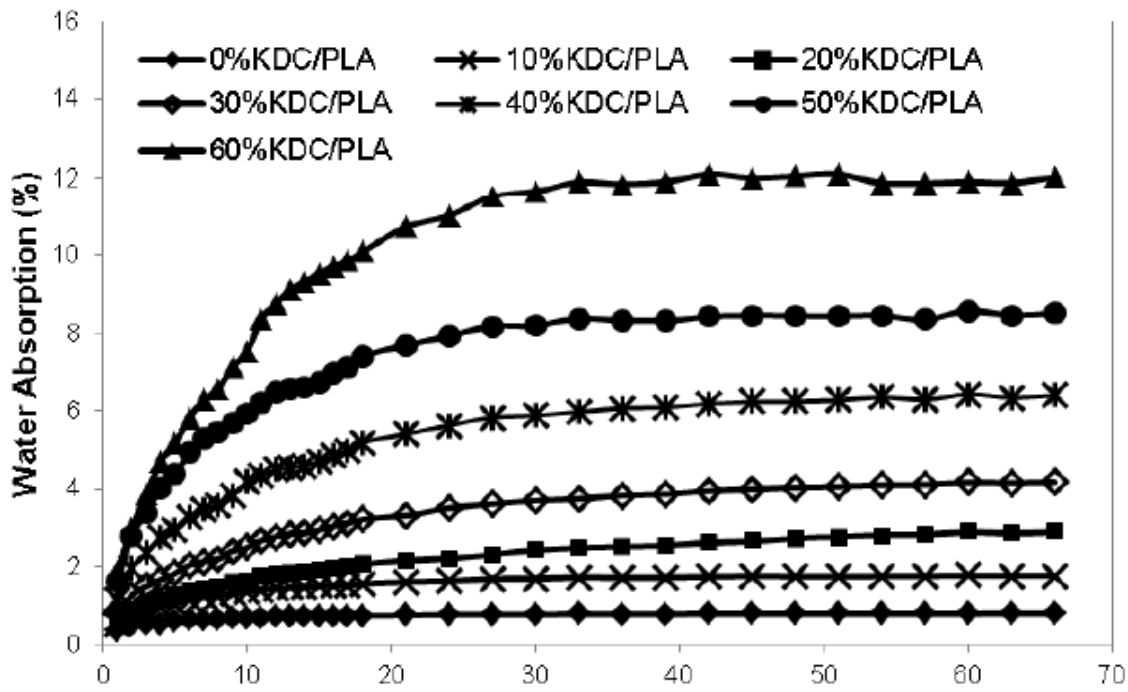


Figure 2.1: The effect of KDC loading on moisture absorption of KDC/PLA composites[9]

achieved the highest impact strength. The figure 2.4 show present of the water absorption of the neat PLA and KDC/PLA composite. The result demonstrate that the water absorption of the neat PLA was lower than that of the KDC/PLA composites.

The influence of KDC was investigated and resulted by the conclusion, the flexural properties of the KDC/PLA composites were improved compared to the those of the commercial neat PLA polymer and the density of the composite increased with KDC content, which may limit its potential applications.[9]

### 2.3 Failure mechanism in dynamic compression

The experiment conducted by (Li, Lu, Jiang, & Fang, 2011) the dynamic stress vs. strain curves and important mechanical properties such as peak stress, modulus and failure strain were determined. Macro fracture morphology and the scanning electron microscope (SEM) micrographs were examined to understand the deformation and failure mechanism of composites. The results show the stress vs. strain curves exhibit obvious non-linear characteristics and a marked softening phenomenon. The composites show clearly the

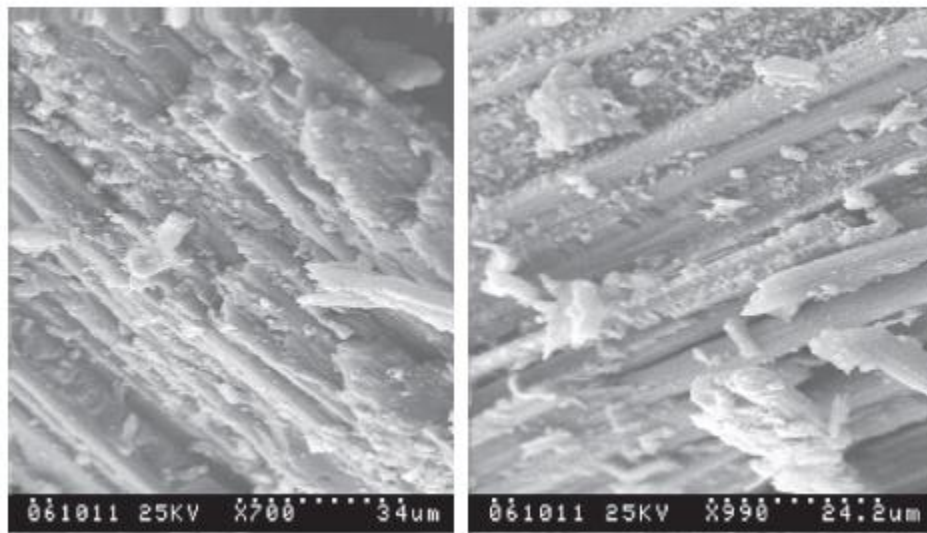


Figure 2.2: The SEM photographs of DTC1 specimen fracture at strain rate of 1150, (a) The interface between the, (b) Matrix plastic deformation fibers and matrix and softened [10]

strain rate strengthening effects and dynamic toughness phenomenon. The damage and failure patterns of composites vary with high strain rates. Moreover, the transverse dynamic compressive properties and failure mechanism can be significantly affected by the braiding angle and the fiber volume fraction. The view of SEM from the researcher as show below figure 2.2. At the higher strain rates exhibit a serious debonding between the fibers and matrix [10]

Work by (Sharba, Leman, Sultan, Ishak, & Azmah Hanim, 2016) the effect of kenaf fiber with different orientation namely, non-woven random mat, unidirectional twisted yarn, and

plain-woven kenaf. The experiment conducted Tensile, compression, flexural, and fully reversed fatigue tests and a morphological study of the tensile failure surface of each hybrid composite was carried out. The monotonic and fatigue properties of kenaf/glass hybrid composites depended on kenaf fiber orientation, which dramatically affected the composite properties. The non-woven random mat kenaf hybrid composite exhibited poor mechanical and fatigue properties compared with the other composites. Its low strain, brittleness, and short fiber length had a noticeable effect on its physical and fatigue properties. These properties lead to the matrix and glass fibers being the main load carriers compared with the kenaf fiber, as shown in Figure 2.3 a). The delamination between the kenaf and the glass was greater and more noticeable than in the other hybrid composites. These observations corroborate the low mechanical properties of the non-woven kenaf hybrid composites. Figure 2.3b depicts the failure surface of the woven kenaf hybrid composite due to tension loading. The different modes of failure were due to high interlocking strength of the wrap and weft yarns. The similarity between the kenaf and glass structure was advantageous for resisting load efficiently. The modes of failure observed in the micrographs show that both the fiber and matrix were the load carriers; this effect can be explained by the existence of matrix cracks, matrix debonding, fiber breakage, less fiber pullout, and less delamination between the fibers. A similar failure behavior was noted in the unidirectional kenaf hybrid composites, but in the axial direction only. Generally, glass fiber was the superior load carrier; micrographs showed the same fiber pullout and fiber-breakage failure modes in all of the hybrid composites. [11]

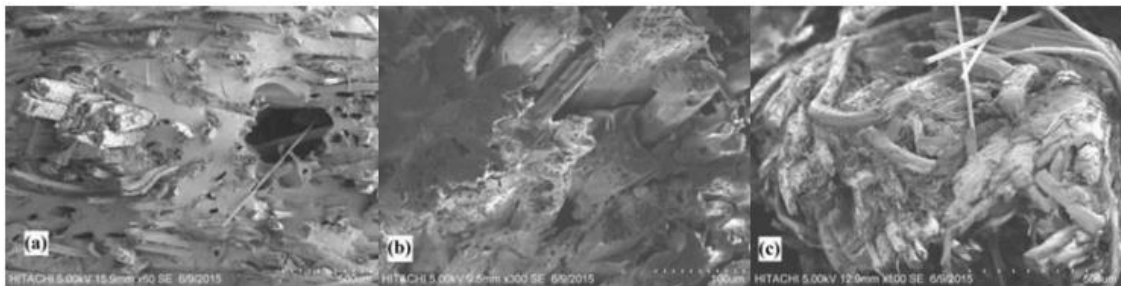


Figure 2.13) Micrographs of tensile failure sections of kenaf hybrid composites: (a) non-woven mat, (b) plain woven, and (c) unidirectional twisted yarns[11]

## **2.4 Concluding remark**

The researcher not conducted experiment dynamic compression on kenaf. Their more focus on static experiment and tensile to find out its properties. The failure mechanism of kenaf also rarely discusses by researcher

## CHAPTER 3

### METRODOLOGY

#### 3.1 Overview

This chapter discusses the step taken into developing this is project successfully. It including the specimen preparation, the testing procedures and failure mechanism determination.

#### 3.2 Material

The specimen used for this experiment was unidirectional 1400 kenaf composite contain of 70 % fiber 30 % matrix (unsaturated polyester crystic 1901) which is obtained from School of Material and Mineral Resources. The specimen was prepared by pultrusion process and cut by using diamond cutter (2000rpm) with diameter 12mm and 6mm length. The size was chosen as suggested by Nakai and Yokoyama, 2008 that the ideal slenderness ratio (height/diameter) for metallic material is 0.5 [12]

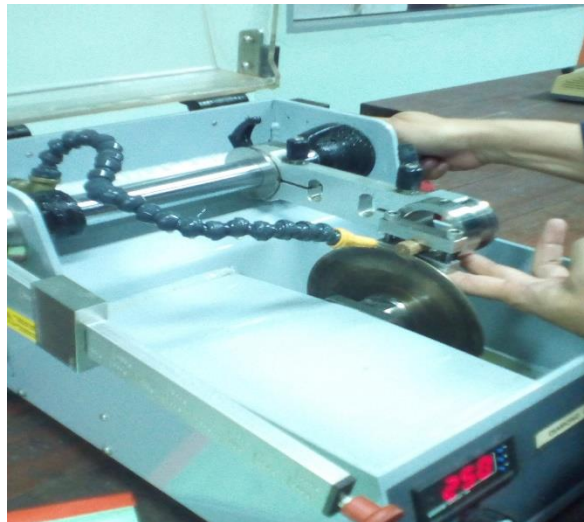


Figure 3.1: The diamond cutter to cut the kenaf with speed 2000rpm



Figure 3.2: Raw result of Strain against Time Graph obtained from SHPB Test

### **3.3 Dynamic test**

The dynamic testing for the high strain rate were conducted by using Split Hopkinson Pressure Bar (SHPB). The apparatus was modified by using momentum trapping to get an accurate result. Typically setup of a SHPB testing rig is made out of a striker which is enhanced by a compressed, a small specimen is crammed between two elastic bars called incident bar and transmission bar, strain gages, a digital storage and strain transducers. All the diameter of the transmission bar, incident bar and the striker are 12 mm respectively and their lengths are both 1500 mm. Both bars are made out of maraging steel that the material with a superior strength and toughness. The density of the maraging steel is  $7800 \text{ kg/m}^3$

#### **3.3.1 Basic principle of Split Hopkinson pressure Bar**

In conventional SHPB technique, the specimen is located in between incident and transmitted bars. To minimize the vibration the wax is applied on each both end of the area of the specimen. The strain rate can be adjusted by changing the gas pressure in the gas tank. For this experiment, the pressurized tank is filled with pressure 1 bar and 3 bar.

Typically when the striker bar accelerated by the pressure and impacts the incident bar, compressive stress pulse is generated and travels along the incident bar towards input bar/specimen. The pulse is partially reflected into the input bar and partially transmitted through the specimen and passes through the transmission bar. The strain gages are mounted on both the incident and the transmitted pulse as function to measure the direct incident pulse, the reflected pulse and the transmitted pulse. The result of the change of voltage and strain will be display in the computer. The experiment repeat three time each bar and conducted in room temperature.

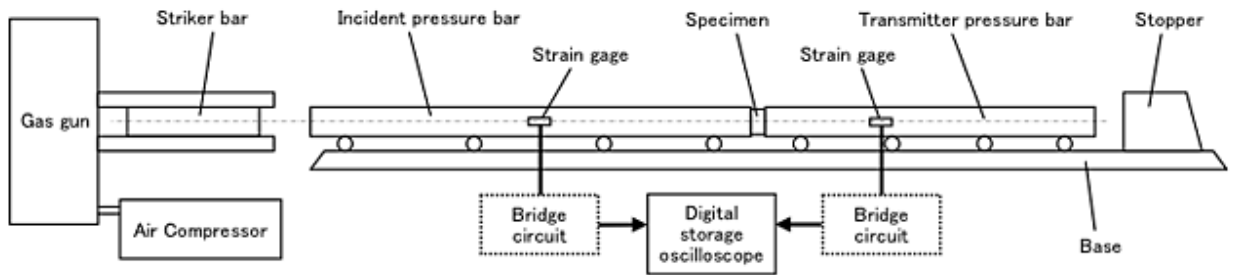


Figure 3.3: The schematic diagram for Split Hopkinson Pressure Bar

### 3.3.2 Theory

The SHPB test will result in a data of voltage and strain which is collected by the strain gages which is mounted on the incident and transmission bar. The typical strain against time and voltage against time obtained from the SHPB test are shown in Figure 3.4 and

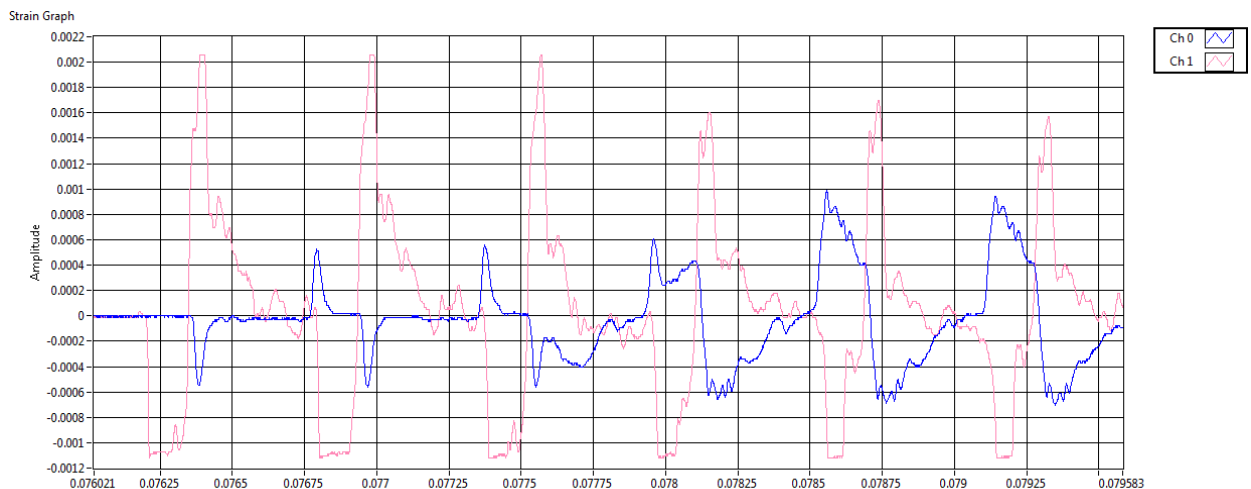


Figure 3.4: Raw result of Strain against Time Graph obtained from SHPB Test





Figure 3.5: Raw result of Voltage against Time obtained from SHPB Test

To obtain the stress, strain rate in the specimen through the graph strain and voltage graph as follows

$$\sigma(t) = -E_b \frac{A_b}{A_s} \varepsilon_t(t)$$

$$\dot{\varepsilon} = 2 \frac{C_0}{L_S} \varepsilon_r(t)$$

$$\varepsilon_s = 2 \frac{C_0}{L_S} \int_0^t \varepsilon_r t (dt)$$

Since,

$$C_0 = \sqrt{\frac{E_b}{\rho}}$$

Where,

$\sigma_s$  = Specimen's Stress

$\varepsilon_s$  = Specimen's Strain

$\dot{\epsilon}$  = Strain Rate

$\epsilon_r$  = Reflected Strain

$L_s$  = Length of Specimen

$C_{0=}$  = Sound wave velocity in Bar

$E_b$  = Young's Modulus of Bar

$A_b$  = Cross-sectional Area of Bar

$A_s$  = Cross-sectional Area of Specimen

$\rho$  = Density of Bar

### 3.3.3 Momentum trap technique

The SPHB was modified by using three parts which are transfer flange, incident tube and reaction mass to achieve an accurate result. The function of transfer flange is the link

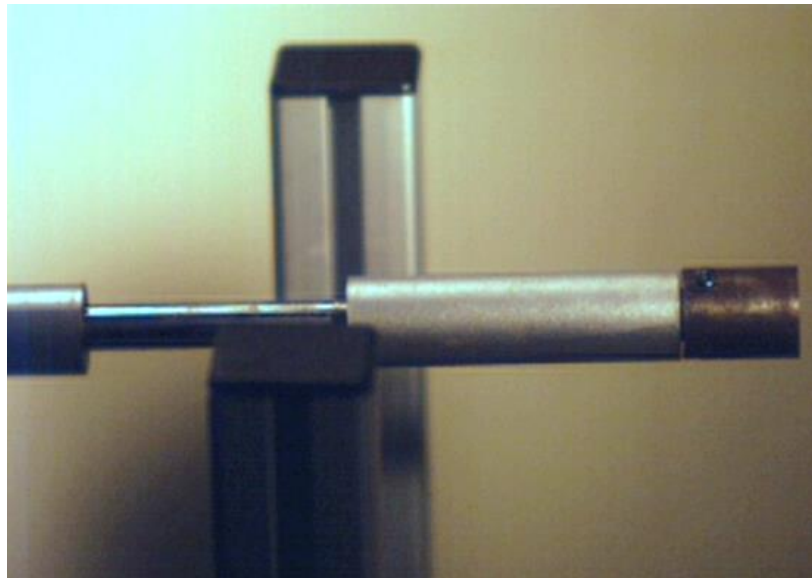


Figure 3.6: The placed of momentum trapping

between of incident bar and incident tube. Incident tube as a stopper to the incident bar and reaction mass as the stopper to the incident tube. The flow of the motion is described below.

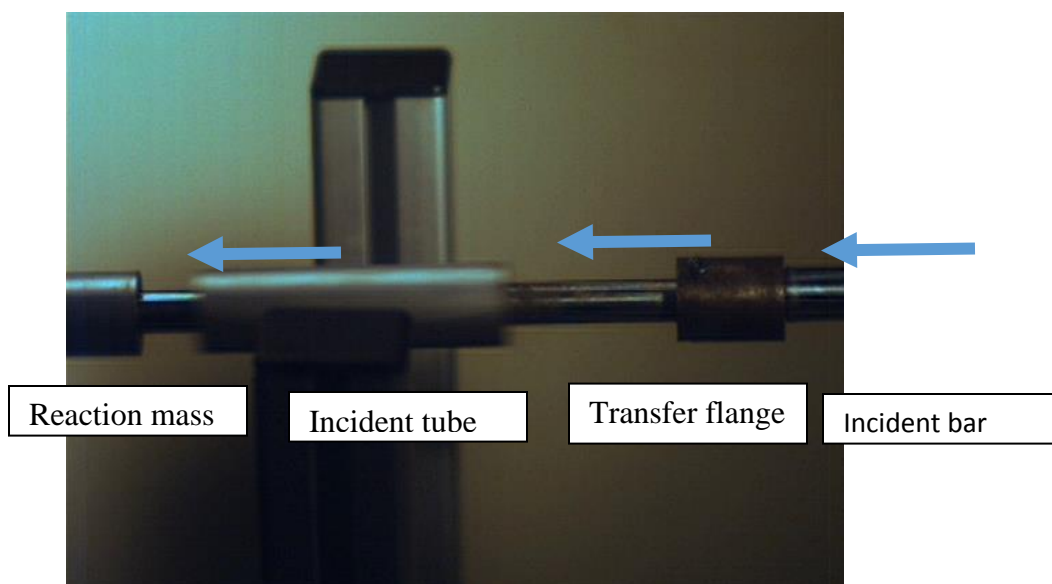


Figure 3.7: The flow of the momentum trapping when the incident tube suddenly hit the transfer flange, the incident tube moving towards the reaction mass.

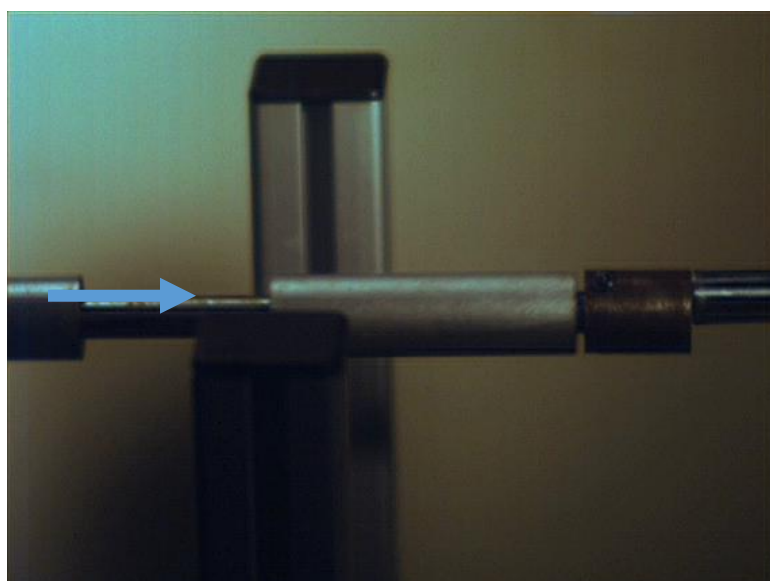


Figure 3.8: The incident tube go back to the original position

### 3.4 Scanning Electron Microscope

The scanning electron microscope Model S-3700N is used in order to verify the failure mechanism of kenaf composites. The scanning electron microscope (SEM) has been recognized as an invaluable tool for observing material surface and fine structure in various fields and industries such as nanotechnology, biotechnology, research, development, and quality control. The simple coating procedure need to follow before proceed to SEM process. Thus about 1.0-1.5 minutes of sputtering will apply enough composite to conduct the SEM electrons to ground and prevent charging without noticeably altering the topography of your substrate. The specimen placed on the stage table after the chamber door of SEM opened. The process of scanning images was run around  $\times 60$  magnification.



Figure 3.7 : The coating process about 1.0-1.5 minutes before proceed with SEM process

Secondary electron image resolution	3.0 nm <b>GUARANTEED</b> (30 kV - HV mode)	
	10.0 nm <b>GUARANTEED</b> (30 kV - HV mode)	
Back Scattered electron image resolution	4.0 nm <b>GUARANTEED</b> (30 kV - LV mode)	
Electron optics	Hitachi patented <b>Quad Bias</b> -function instead of expensive LaB <sub>6</sub> -tips	STANDARD
Electron gun	Tungsten Emitter (Filament-change within 20 minutes)	
Accelerating Voltage	0.3 - 30 kV	
Magnification	5X - 300.000X	
	RELATED to POLAROID (4" X 5")	
Objective aperture	5-Positions, Click Stop Objective Aperture	
Detector system	Everhardt Thornley <b>Secondary Electrons (SE) Detector</b>	STANDARD
	High Sensitivity Semiconductor <b>BSE Detector - 4+1-Segment</b>	STANDARD
	Energy Dispersive X-ray Spectrometer (EDX)	OPTION
	FF Wavelength Dispersive X-ray Spectrometer (WDX)	OPTION
	Electron Back Scattered Diffraction-Analyzer (EBSD)	OPTION
	Cathode Luminescence Spectrometer (CL)	OPTION

	<b>Environmental SE Detector ESED II (2.GENERATION!!!)</b>	OPTION
	X-ray source	OPTION
Low Vacuum Range	6 - 270 Pa	
Image Shift	$\pm 50\mu\text{m}$ at WD = 10mm	
Specimen stage	X = 0 - 150 mm	
	Y = 0 - 110 mm	
	Z = 5.0 - 65 mm	
	R = 360°	
	T = -20° - +90°	
	Maximum Height = <b>110mm</b>	
	Observable area in diameter = <b>203 mm</b> with Rotation	
	Maximum specimen size in diameter = <b>300 mm</b>	
Image display	PC with Operating system Windows XP	STANDARD
	One or two 19" LCD-FLAT-PANEL	STANDARD
	640 x 480 up to 5.120 x 3.840 pixel	STANDARD
	Multiple Image formats (JPG/TIFF/BMP)	STANDARD
	<b>Signal Mixing - Fully selectable Detector signals</b>	STANDARD
	Dual Image Display	STANDARD

Table 3.1: The specification of scanning electron microscope Model S-3700N



Figure 3.8: The images of Scanning Electron Microscope Model S-3700N

### 3.5 High speed camera

By using Olympus high speed camera 2, the movement of the dynamic compression was captured by the highest resolution. The resolution used for this experiment about 1000rps. The camera was set up in front of specimen that located between incident bar and transmission bar. From the images obtained, learn a great deal about motion sequences if we record them with high speed video cameras and then study the recordings in slow motion


Picture	Description
	<p>Resolution (full sensor) : 800 x 600 pixels</p> <p>Speed at full resolution : 1,000 fps</p> <p>Maximum recording speed : 33,000 fps</p>

Table 3.2: The description of high speed camera 2

## CHAPTER 4

### RESULT AND DISCUSSION

#### 4.1 Overview

In this section, the strain- time data recorded from the data acquisition were manipulated. The raw data were processed to obtain the stress-strain curves at different strain rate by using the formula in equation at chapter 3. The morphology view for the failure was investigated by using Scanning Electron Microscope.

#### 4.2 Stress-Strain Graph

Figure 4.1 represents the oscilloscope records from the compression SHPB test on Kenaf fibre. The strain graph versus time were represented after the compression testing. Normally, the strain rate is obtained from the initial slope of the figure 4.1. The Nakai and Yokoyama [12] has suggested that the strain rate is calculated by dividing the area under the strain rate strain curve up to maximum strain under loading by the maximum strain and other work by Kaiser [13] also employed a similar approach. As a result, the strain rate recorded during the SHPB test is  $1733s^{-1}$ . The maximum failure stress and maximum failure strain were obtained by using equation discussed before.



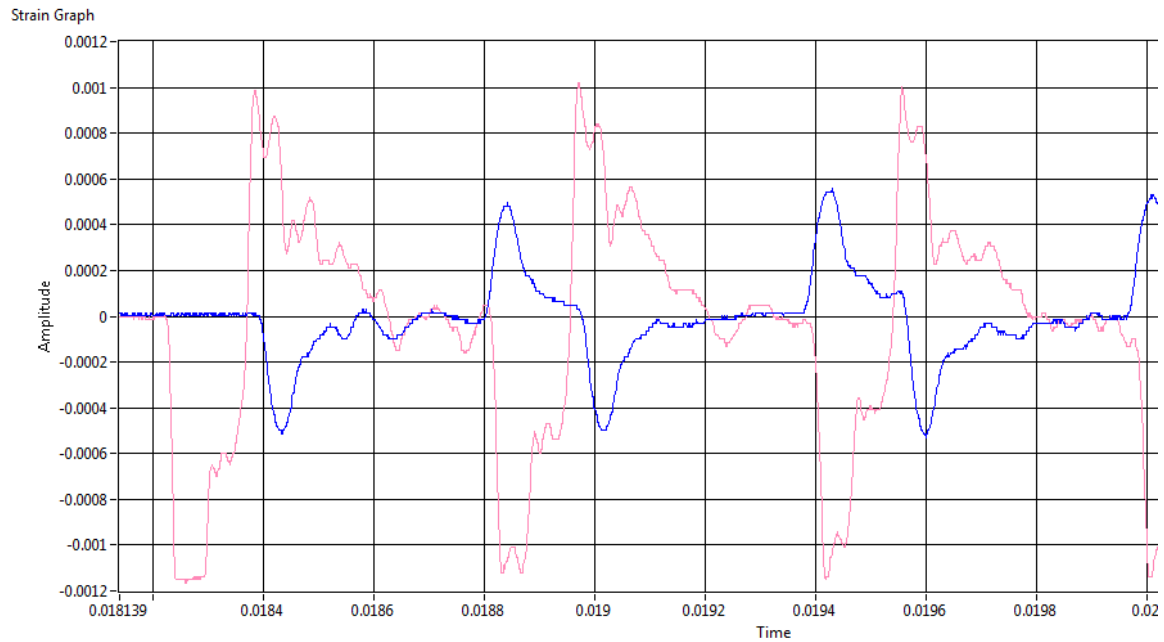


Figure 4.1 : The example of raw data for the  $1733s^{-1}$

A representative of five results at different strain rate is shown in figure 4.2 to analyze the behavior of kenaf until it failure. The value of the maximum strain, maximum stress, and strain rate is presented in Table 4.1. The curve exhibit nonlinear characteristic with modulus increased in increasing strain rate. When the failure starts, the sample is no longer in a state of homogenous deformation, and the valid range of experiment is over [14]. Noticeably, the stress increase drastically as the strain rate increase. From the data above, the stress-strain curve, the higher strain rate have a faster time to failure and the graph steeper than others. There was considerable increase in the toughness and peak stress values of the composite with increasing strain rate during high-strain-rate loading. But the strain at peak stress was found to be decreases. The increase in stress can be directly related to the secondary molecular processes and their explaining on this phenomenon [15-16]. Besides, the increasing strain rate will decrease the molecular mobility of the polymer chains and thus make material stiffen [17]

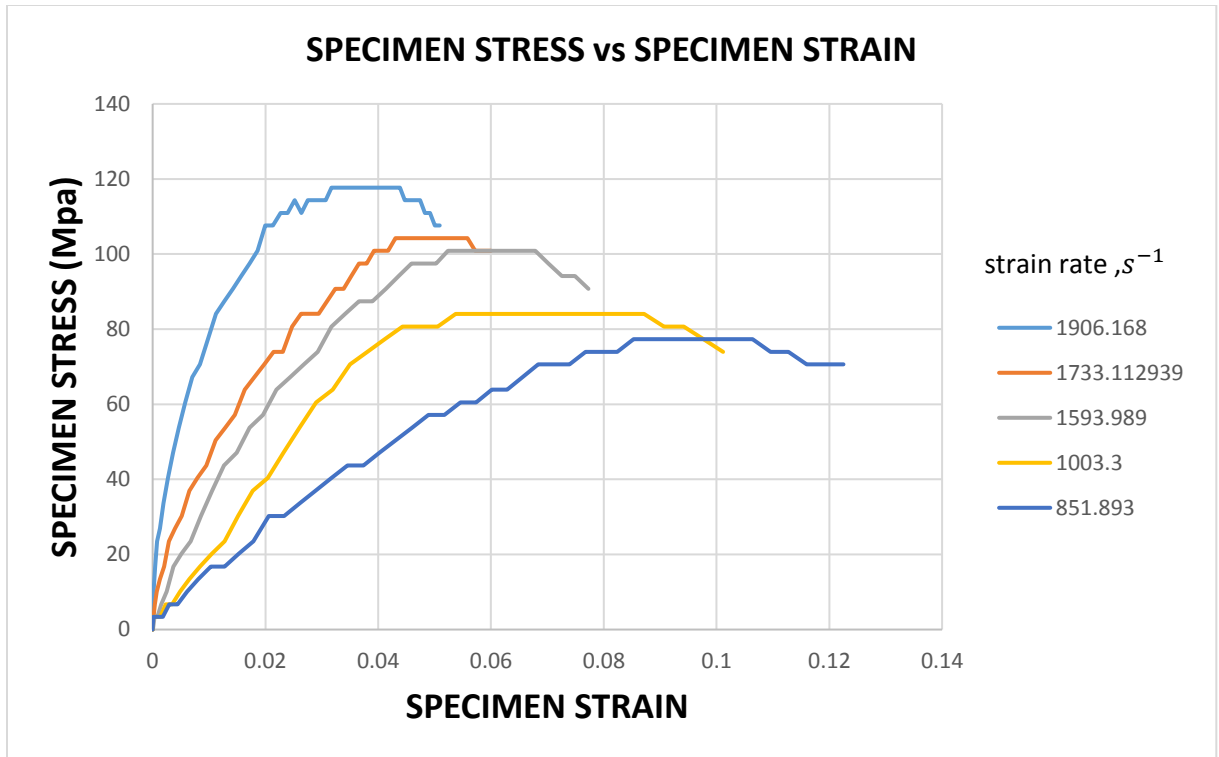


Figure 4.2: The stress-strain graph with different strain rate

TIME	STRAIN RATE	MAXIMUM STRESS	MAXIMUM STRAIN
0.053124	851.9	77.33565	0.085266431
0.036835	1003.3	84.061	0.05375
0.030528	1593.989	100.87539	0.050262458
0.018989	1733.113	104.23812	0.04304308
0.01274	1906.168	117.68925	0.031692723

Table 4.1: The detail properties for the compression testing

### 4.3 Effect of strain rate

The data of the experiment were plotted by failure strain-stress rate and failure stress-strain rate graph.

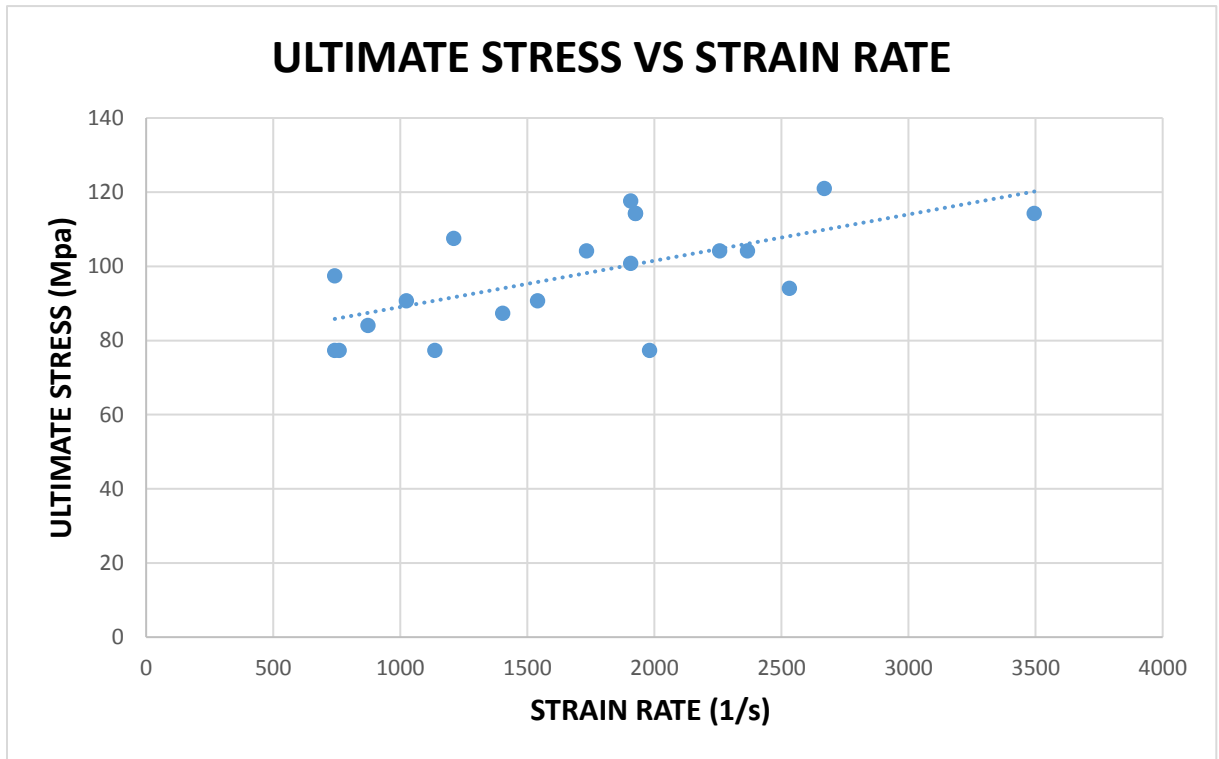


Figure 4.3: The failure stress specimen with different strain rate